International Information and Engineering Technology Association

Advancing the World of Information and Engineering

Optimal Configuration of a Solar Heating System with Seasonal Thermal Energy Storage Serving a Micro-scale Italian Residential District: Energy, Environmental and Economic Analyses

Check for updates

Antonio Rosato, Antonio Ciervo*, Giovanni Ciampi, Michelangelo Scorpio, Sergio Sibilio

Department of Architecture and Industrial Design, University of Campania "Luigi Vanvitelli", 81031 Aversa (CE), Italy

Corresponding Author Email: antonio.ciervo@unicampania.it

ABSTRACT

A centralized solar hybrid heating system serving a micro-scale district composed of 6 typical Italian residential buildings and 3 schools located in Naples (southern Italy) has been modelled, simulated and analyzed by means of the dynamic software TRNSYS over a 5-year period. The plant is based on the operation of solar thermal collectors connected to a seasonal single U-pipe vertical Borehole Thermal Energy Storage (BTES) in order to address the seasonal misalignment between solar energy supply and thermal energy demand for heating purposes. In this paper, a parametric analysis has been performed in order to investigate the performance of the plant upon varying the characteristics of the BTES in terms of: (i) thermal conductivity of soil, (ii) thermal conductivity of grout, (iii) U-pipe spacing, (iv) heat carrier fluid, (v) number of Borehole Heat Exchangers (BHEs), as well as (vi) type of BHEs connection (series, parallel or mixed). The primary energy consumption, the equivalent carbon dioxide emissions and the operating costs of the proposed district heating network have been evaluated based on the simulation results upon varying the plant configurations and then compared with those associated to a conventional Italian decentralized heating system assumed as reference in order to (i) assess the potential benefits, (ii) explore the influence of BTES configuration on the overall system performance, and (iii) establish some simple rules for the initial phase of BTES design.

1. INTRODUCTION

District Heating Systems (DHSs) are characterized by a number of advantages with respect to conventional decentralized heating plants [1]. The European Directive 2012/27 [2] calls for the presence of a renewable share inside the so-called "efficient district heating and cooling". Among the renewable energy sources, an increased use of solar energy can be credited to worldwide trends and legislative incentives directed to resolving environmental issues. However, one of the longstanding barriers to solar energy technology lies in the noticeable seasonal misalignment between solar energy supply and thermal energy demand. Long-term storages allow for thermal energy storage over weeks and months, with they being a challenging key technology for solving this time-discrepancy [3-5]. Sensible seasonal heat storage is a comparatively mature technology in which water, rock-sort material and/or ground/soil are frequently used as storage materials [3-5]. There are four main types of sensible seasonal energy storage in operation [3-5]; based on a comprehensive literature review, Rad and Fung [1] concluded that Borehole Thermal Energy Storage (BTES) has the most favorable condition for long-term energy storage thanks to the large amounts of energy involvement and relatively low cost of storage media. BTESs consist of closed-loops where heat is charged or discharged by vertical or horizontal Borehole Heat Exchangers (BHEs), which are installed into boreholes with a depth up to 100 m below the ground surface. After drilling, a "U" pipe is inserted into the borehole; in order to enhance the

thermal contact with the surrounding soil, the borehole is then filled with a high thermal conductivity grouting material. BHEs can be single or double U-pipes; a certain number of BHEs can be hydraulically connected in series to a row and a certain number of rows can be connected in parallel. The so-called Central Solar Heating Plants with Seasonal Storage (CSHPSS), i.e. district heating systems based on the exploitation of solar source and integrated with long-term thermal energy storage, are gaining more and more attention as a very promising alternative to fossil fuel heating [5] and they have been researched by several entities, such as IEA's Task 32 and Task 45 [6, 7], as well as the German programme Solarthermie [8]. Numerous CSHPSS projects have seen the light of day in Europe and North America [5], both on large and small scales. All studies [1, 3-5] came to the conclusion that CSHPSS can play a significant role in the implementation of future smart energy systems, even if future researches are needed [5]. One of the main factors of concern for the design of future CSHPSSs is the energy storage, considering that an oversized system or a system with an insufficient number of boreholes will lead to an increase in costs and losses [9, 10]. The performance of a BTES is greatly affected by its geometry, thermo-physical properties of both soil and grout, temperature and mass flow rate of heat carrier fluid, etc. Several papers focusing on BHEs deal with the influence of one or more of these parameters, but the literature review reveals that global studies assessing the impact of BTES design on the overall energy, environmental and economic performance of small-scale solar district heating systems are not available. A limited

number of studies have been performed with reference to solar district heating systems under Italian climatic conditions and the integration of seasonal thermal energy storages has been rarely considered [11-16]. In addition, most of these works performed an energy analysis in terms of solar fraction as well as primary energy savings, without considering the emissions as well as the economic performance. Finally, it should be noticed that districts with a size much larger than that one considered in this study have been analyzed in the above-motioned works. This justifies the need to perform additional investigations for Italian applications. In this paper, a solar hybrid district heating system is modelled, simulated and analyzed by means of TRNSYS 17 [17] over a 5-year period. The proposed plant is based on the operation of solar thermal collectors connected with both a short-term thermal energy storage (STTES) as well as a seasonal single U-pipe vertical Borehole Thermal Energy Storage (BTES). The system is aimed at satisfying the heating demand and domestic hot water requirements of a micro-scale district composed of 6 Italian typical single-family houses under the climatic conditions of Naples (southern Italy). In a previous study [18], the authors investigated the performance of the proposed plant upon varying the following parameters: (i) area of solar thermal collectors, (ii) volume of STTES, (iii) volume of BTES. In this work the performance of the optimal plant configuration, previously identified by the authors on the basis of the simulation results of a huge parametric analysis [18], are further investigated in more detail upon varying the characteristics of the BTES in terms of (i) thermal conductivity of soil (0.5, 1.5 and 3.0 W/mK), (ii) thermal conductivity of grout (0.5, 1.3 and 5.0 W/mK), U-pipe spacing (0.0254, 0.0350 and 0.0500 m), heat carrier fluid typology (mixture of water and ethylene glycol or pure water), number of BHEs (2, 4, 6, 8 and 10 BHEs), type of BHEs connection (series, parallel or mixed). A total of new 67 simulation cases are analyzed in this study. The primary energy consumption, the equivalent CO_2 emissions and the operating costs associated to each plant configuration are then compared with those associated to a typical Italian decentralized heating system assumed as reference in order to (i) assess the potential benefits, (ii) explore the influence of BTES configuration on the overall system performance, and (iii) establish some simple rules for the initial phase of BTES design.

2. DESCRIPTION OF THE DISTRICT

The district served by the proposed plant is composed of 6 typical Italian single-family residences located in Naples (south of Italy; latitude = 40° 51' 46" 80 N; longitude = 14° 16' 36" 12 E; Heating Degree-Days = 1,034). Three different typologies of residential buildings (A, B and C) have been considered (with 2 residential buildings for each typology). Table 1 summarizes the main characteristics of the buildings composing the district.

Table 1. Main characteristics of residential buildings

	Type of buildings		
	A	B	C
Number of buildings (-)	2	2	2
Floor area (m²)	60	78	114
Windows' area (m²)	84	102	230
Volume (m³)	230	370	448
Maximum number of occupants (-)	3	4	5

In order to be compliant with Italian legislation requirements, the thermal transmittance of the buildings' envelopes has been equated to the given threshold values (2.40 W/m²K for windows, 0.36 W/m²K for roofs, 0.40 W/m²K for floors, 0.38 W/m²K for external vertical walls), whatever the building typology is. For each residential building typology, a specific annual stochastic profile (composed of 365 different daily stochastic profiles) at one-minute time resolution has been considered for determining the occupancy as well as the electric demand associated to both lighting and domestic appliances; these annual stochastic profiles have been obtained by using the models developed by Richardson and Thomson [19]. A total annual electric energy demand for the 6 residential buildings of 14.98 MWh/y has been derived. Several sets of yearly load profiles for the domestic hot water demand have been specified within the IEA-SHC Task 26 [20]. In this study, a demand profile with an average basic load of 100 L/day in the time scale of one minute has been used for both residential building typologies A and B, while a demand profile with an average basic load of 200 L/day in the time scale of one minute has used for residential building typology C. The maximum thermal demand for space heating is about 28.2 kW (typology C of residential buildings), while the maximum thermal load for DHW production is about 37.5 kW (typology C of residential buildings); the maximum electric demand of the residential buildings is about 5.8 kW (typology C of residential buildings).

3. DESCRIPTION OF THE PROPOSED DISTRICT HEATING SYSTEM

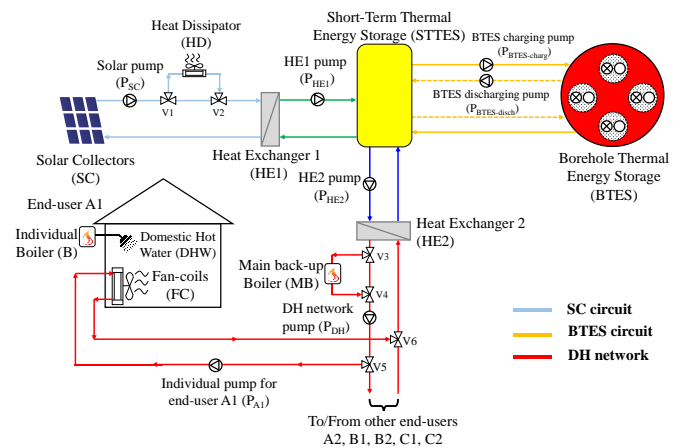The schematic of the proposed CSHPSS is reported in Figure 1.

Figure 1. Schematic of the proposed central solar heating plant with seasonal thermal energy storage (CSHPSS)

In this figure, the following main components of the system can be identified: end-users (6 residential buildings A1, A2, B1, B2, C1, C2), solar thermal collectors (SC), heat dissipator (HD), short-term thermal energy storage (STTES), borehole thermal energy storage (BTES) with vertical single U-pipes borehole heat exchangers, main natural gas-fired back-up boiler (MB), heat exchangers (HE1 and HE2), local individual boilers (B) for DHW production, fan-coils (FC), pumps (P), 3-way valves (V) and pipes. The following three main circuits are highlighted: SC circuit, BTES circuit and district heating (DH) network. The solar energy captured by the SCs is first

transferred, through the HE1, into the STTES; dissipation of solar energy surplus is obtained by blowing air across a finned coil heat exchanger (HD) when the temperature at the outlet of solar field is higher than 95°C. From the STTES, if there is a heating demand, the solar energy is transferred through the HE2 into the distribution network, and then to the end-users for space heating; every building is equipped with a group of fan-coils, supplied by the STTES. If the solar energy is not immediately required for heating purposes, it can be moved from the STTES to the BTES system during the whole year ("BTES charging mode"): in this case, the heat carrier fluid is taken at the top of STTES, circulated through the BTES and then re-entered at the bottom of the STTES. Only during the heating season, thermal energy stored in the BTES field can return into the STTES ("BTES discharging mode") to eventually integrate the temperature level into the STTES. During the charging mode, the flow direction is from the center to the boundaries of the BTES to obtain higher temperatures in the center and lower ones at the boundaries of the storage; the flow direction is reversed during the discharging phase. A main natural gas-fired boiler (MB) is used to supplement the space heating demand when the solar energy collected and stored in the STTES and BTES cannot meet the energy requirements. An individual natural gas-fired boiler has also been installed inside each residential building specifically devoted to the domestic hot water production. All the electric requirements are satisfied with the electric energy supplied by the central national grid. The main characteristics of each component of the proposed CSHPSS are indicated in Table 2.

3.1 Simulation models

In the TRaNsient SYStems (TRNSYS) software platform [17] each physical piece of the thermodynamic equipment is modeled with a component (named "Type" in TRNSYS terminology). TRNSYS Types have been selected from the TRNSYS libraries and enhanced by manufactures performance data or information available in the current scientific literature. The duration of simulation period (5 years) has been defined in order to consider that it takes time to fully charge the seasonal storage. January 1st has been assumed as starting date of the simulations. A simulation time step of 1 minute has been adopted.

Table 2. Main characteristics of CSHPSS components

Solar thermal collectors (SC) [21]	
Collector technology / model	Flat plate / FSK 2.5
Gross / Aperture area of a single collector (m^2)	2.51 / 2.31
Number of collectors	24 (8 rows with 3 series-connected panels per row)
Tilted angle / Azimuth / Orientation	30° / 0° / South
Short-term thermal energy storage (STTES) [22]	
Volume (m^3) / Height (m)	6.0 / 3.5
Boreholes thermal energy storage system (BTES)	
BTES volume (m^3) / Borehole radius (m)	435.8 / 0.15
Inner / Outer radius of U-pipe (m)	0.01372 / 0.01664
Pipe / Gap thermal conductivity (W/mK)	0.42 / 1.40
Main back-up boiler (MB) [23]	
Fuel / Rated capacity (kW)	Natural gas / 26.6

Type 56 has been used to model the thermal behavior of the buildings composing the district. The Type 557a [24], adopted to model the BTES, is considered to be the state-of-the-art in dynamic simulation of ground heat exchanger that interacts thermally with the ground and has been used by several researchers for simulating energy systems with BTES. The storage volume has the shape of cylinder with vertical symmetry axis; within this cylindrical storage volume, the ground is considered to be homogeneous. The layout of the borehole field is fixed hexagonally and uniformly within the storage volume in the simulation. The Type 534 used to model the STTES is based on the assumption that the tanks can be divided into fully-mixed equal sub-volumes. In this paper, the STTES has been modeled with 10 isothermal temperature layers to better represent the stratification in the tank, where the top layer is 1 and the bottom layer is 10. The model has been calibrated based on manufacturer data [22]. Flat-plate solar thermal collectors have been modeled using TRNSYS Type 1b. In this component model, the collector efficiency (η_{SC}) has been modeled by a second-order equation (Eq. 1), and correction for off-normal solar incidence is applied by a second-order incidence angle modifier (K) equation (Eq. 2):

$$\eta_{SC} = 0.7484 - 16.17 \cdot \left(T_{in,SC} - T_a\right)\big/G \tag{1}$$

$$K = 1 - 0.103 \cdot S \tag{2}$$

where, $T_{in,SC}$ is fluid inlet temperature, T_a is ambient temperature, G is solar radiation and $S=1/\cos\theta$-1 (θ is the incident angle for beam radiation). The coefficients (in SI units) listed in Eqs. 1-2 have been based on manufacturer data for a single flat-plate collector [21]. The counter flow plate heat exchangers HE1 and HE2 have been modeled with the TRNSYS Type 5b by assuming an overall heat transfer coefficient equal to 25 W/K per GJ of the heat demand for HE1 and 54.3 W/K per m^2 of collector areas for HE2, respectively, according to the values suggested by Pahud [25]. The main boiler has been modeled by TRNSYS Type 700; a rated capacity of 26.6 kW has been assumed. The MB is able to modulate the thermal output between 40 % and 100 % of its rated capacity, with an efficiency varying upon varying the thermal output $P_{th,out,MB}$ according to the following equation (based on manufacturer performance data [23]):

$$\eta_{MB} = 0.0015 \cdot P_{th,out,MB} + 0.8814 \tag{3}$$

Individual boilers installed inside the houses for DHW production have been modeled through TRNSYS Type 700 by assuming a rated capacity of 26.6 kW per each, with a constant efficiency equal to 90 %. Fan-coils have been modeled by TRNSYS type 753d. It has been calibrated based on manufacturer performance data. The heat dissipator is simulated by considering TRNSYS Type 511, that models a device used to cool a liquid stream by blowing air across coils containing the liquid. A distribution network with a single pair of supply and return pipes has been used for both the distribution network as well as the solar field collector circuit. TRNSYS type 31 has been used to model the pipes and calculate the related heat losses by assuming a loss coefficient equal to 0.05 kJ/hm^{2}K. The DH network pump has been modeled by TRNSYS Type 742, while all the other pumps in the system have been modeled by TRNSYS Type 656. A

specific EnergyPlus weather data file [26] has been considered for modeling the weather conditions of Naples; the weather data are one-year long and, therefore, have to be the same each year.

3.2 Control logics

The duration of the heating period has been assumed from 15th November up to 31st March. The heat carrier fluid flows through the fan-coils only in cases when there is a call for heat triggered by a thermostat installed in each building. The room temperature is targeted to be kept at 20 °C only in the case of at least one occupant being inside the building, otherwise the indoor air temperature is not controlled. When the room temperature is lower than 19.5 °C, it calls for heat from the STTES; the call for heat signal will be disabled when the room temperature reaches 20.5 °C. The set-point for the DH supply temperature is 55 °C, so that the target of the main back-up boiler thermostat is fixed at 55 °C with a dead band of 5 °C. The DH network pump operates continuously with a flow rate varying between 497.7 kg/h and 3,782.7 kg/h (depending on the number of buildings requiring thermal energy for space heating) during the heating season. Even if there is no heat demand, the DH network pump operates with the minimum flow rate to avoid a significant temperature drop in the district heating network; the flow rate on the source side of the heat exchanger HE2 is set to the same value of the load side. The solar energy recovery is based on the comparison between the current values of the temperature at node 10 (lower part) of the STTES and the temperature of the fluid exiting the solar field. The BTES charging/discharging is controlled based on the current values of the temperature at nodes 1 (upper part) and 10 (lower part) of the STTES, the temperature in the center of BTES field as well as the room target temperature (20 °C). In more detail, during the BTES charging mode, the flow rate, which is constant, is set to half of the nominal flow rate in the collector array; in the BTES discharging mode, the flow rate is set to the current value used in the distribution network. The DHW is assumed to be produced at 45 °C. Table 3 reports the control strategies for activating/deactivating the main components of the proposed CSHPSS.

4. DESCRIPTION OF THE REFERENCE HEATING SYSTEM

A conventional Italian decentralized heating system (CS) has been modeled and simulated to be compared with the proposed CSHPSS while serving the same district composed of 6 residential buildings (Table 1). In the reference heating system, each building is equipped only with a natural gas-fired boiler (characterized by a constant thermal efficiency of 90 % with a rated capacity of 26.6 kW) used for both space heating purposes (through a group of fan-coils installed inside the buildings) and domestic hot water production. The heat carrier fluid flows through the fan-coils only in cases when there is a call for heat triggered by a thermostat installed in each building. The room temperature is targeted to be kept at 20 °C (with a dead band of 1 °C) only in the case of at least one occupant being inside the building, otherwise, the indoor air temperature is not controlled (as in the proposed CSHPSS). The set-point of the individual boilers is 55 °C for heating purposes, with a dead band of 5 °C. The occupancy, electric and DHW demand profiles used for the proposed CSHPSS

have been also assumed for the residential buildings served by the reference heating system. As in the proposed CSHPSS, the DHW is assumed to be produced at 45 °C. All the electric requirements are satisfied with the electric energy supplied by the central national grid (as in the proposed CSHPSS).

Table 3. Control strategies of proposed CSHPSS

	ON	OFF
Solar pump & HE1 pump	$(T_{SC,out} - T_{10,STTES}) \geq 10$ °C AND $T_{1,STTES} \leq 90$ °C	$(T_{SC,out} - T_{10,STTES}) \leq 2$ °C OR $T_{1,STTES} > 90$ °C
BTES pumps (charging and discharging)	***CHARGING MODE*** *Heating period:* $(T_{10,STTES} - T_{room,set-point}) \geq 10$ °C AND $T_{1,STTES} \geq 60$ °C AND $(T_{1,STTES} - T_{BTES,center}) \geq 10$ °C	***CHARGING MODE*** *Heating period:* $(T_{10,STTES} - T_{room,set-point}) \leq 2$ °C OR $T_{1,STTES} \leq 55$ °C OR $(T_{1,STTES} - T_{BTES,center}) \leq 2$ °C
	Cooling period: $(T_{1,STTES} - T_{BTES,center}) \geq 10$ °C	*Cooling period:* $(T_{1,STTES} - T_{BTES,center}) \leq 2$ °C
	DISCHARGING MODE *Heating period:* $(T_{BTES,center} - T_{10,STTES}) \geq 5$ °C AND $T_{1,STTES} \leq 60$ °C	***DISCHARGING MODE*** *Heating period:* $(T_{BTES,center} - T_{10,STTES}) \leq 2$ °C OR $T_{1,STTES} > 65$ °C
DH network pump	Heating period	Cooling period
Individual pumps & Fan-coils	Heating period AND $T_{room} < 19.5$ °C	Cooling period OR $T_{room} > 20.5$ °C
HE2 pump	Heating period AND DH network pump ON AND $(T_{in,HE2,hot} - T_{in,HE2,cold}) \geq 5$ °C	Cooling period OR DH network pump OFF OR $(T_{in,HE2,hot} - T_{in,HE2,cold}) \leq 2$ °C
Main boiler	Heating period AND $\dot{m}_{FC} > 0$ AND $T_{in,MB} < 50$ °C	Cooling period OR $\dot{m}_{FC} = 0$ OR $T_{out,MB} \leq 55$ °C
Individual boilers for DHW production	$\dot{m}_{DHW} > 0$ AND $T_{in,B} < 45$ °C	$\dot{m}_{DHW} = 0$ AND $T_{out,B} \leq 45$ °C

5. METHODS OF ANALYSIS

The total aperture area of solar collectors (55.4 m^2), the volume of STTES (6.0 m^3) as well as the volume of BTES (435.8 m^3) have been determined by the authors based on the results of a huge sensitivity analysis performed in a previous study [18] where the following parameters have been varied:

$$\text{SCA} = \frac{\text{Gross solar collectors area}}{\text{Annual space heating demand}} \quad (4)$$

$$SSV = \frac{\text{Short-term thermal energy storage volume}}{\text{Annual space heating demand}} \qquad (5)$$

$$SLV = \frac{\text{Long-term thermal energy storage volume}}{\text{Gross solar collectors area}} \qquad (6)$$

In particular, 3 different values of SCA (2.21, 3.32, 4.42 m^2/MWh), SSV (0.2, 0.4, 0.7 m^3/MWh) and SLV (1.8, 3.6, 7.2 m^3/m^2) have been analyzed by the authors in [18] by simulating 27 plant configurations; the variation ranges of SCA, SSV and SLV have been defined based on the design guidelines suggested by Pahud [25] as well as according to the characteristics of commercial products available on the market [18]. The simulation results associated to the configurations corresponding to the above-mentioned values of SCA, SSV and SLV have been compared with those associated to a conventional heating system in terms of primary energy, CO_2 equivalent emissions and operating costs. The comparison highlighted that the best case in terms of primary energy saving is the case characterized by SCA = 4.42 m^2/MWh, SSV = 0.4 m^3/MWh and SLV = 7.2 m^3/m^2, with a total of 4 BHEs (two boreholes connected in series to a row and two rows connected in parallel) characterized by a depth of 24.9 m.

Taking into account that the borehole thermal energy storage is a key component for optimizing the overall performance of the solar district heating system, in this paper additional 54 configurations have been investigated by varying the following parameters: (i) thermal conductivity of soil λ_{soil} (0.5 W/mK, 1.5 W/mK, 3.0 W/mK); (ii) thermal conductivity of grout λ_{grout} (0.5 W/mK, 1.3 W/mK, 5.0 W/mK); (iii) U-pipe spacing (0.0254 m, 0.0350 m, 0.0500 m); (iv) heat carrier fluid (mixture of water and ethylene glycol (60 %/40 % by volume) or pure water). The variation ranges of thermal conductivity of soil, thermal conductivity of grout and U-pipe spacing are defined based on information available in the current literature [27]; in particular, in [27] it is stated that the values of λ for the grouting material can vary between 0.5 and 5.0 W/mK, while the thermal conductivity of soil is in the range 0.5÷3.0 W/mK. Table 4 describes the corresponding 54 simulation cases analyzed in this study and characterized by SCA= 4.42 m^2/MWh, SSV = 0.4 m^3/MWh and SLV = 7.2 m^3/m^2, with a total of 4 BHEs (two boreholes connected in series to a row and two rows connected in parallel) characterized by a depth of 24.9 m.

The energy, environmental and economic analysis of the 54 configurations described in Table 4 allowed to identify the simulation case 27 as that one characterized by the best performance in the case of the mixture of water and ethylene glycol is used. Starting from this configuration, additional simulations have been carried out in this paper in order to analyze the impacts of both (a) the number of BHEs (2, 4, 6, 8, 10 BHEs have been considered) as well as (b) the BHEs connection (series-connected, parallel-connected, mixed connection). In more detail, the plant configurations described in Table 5 have also been simulated and analyzed; they are characterized by the same following design parameters: SCA = 4.42 m^2/MWh, SSV = 0.4 m^3/MWh, SLV = 7.2 m^3/m^2, thermal conductivity of soil = 3.0 W/mK, thermal conductivity grout = 5.0 W/mK, U-pipe spacing = 0.0500 m, and heat carrier fluid (mixture of mixture of water and ethylene glycol).

In the next sections the methods of energy, environmental and economic analyses used in this study are detailed.

Table 4. Matrix of 54 simulation cases upon varying the thermal conductivity of soil and grout, U-pipe spacing and heat carrier fluid (2 parallel-connected BHEs + 2 series-connected BHEs with a depth of 24.9 m)

Simulation cases	λ_{soil} (W/mK)	λ_{grout} (W/mK)	U-pipe spacing (m)	Heat carrier fluid
1	0.50			
2	1.50	0.50		
3	3.00			
4	0.50			
5	1.50	1.30	0.0254	
6	3.00			
7	0.50			
8	1.50	5.00		
9	3.00			
10	0.50			
11	1.50	0.50		mixture of water and ethylene glycol (60 %/40 % by volume)
12	3.00			
13	0.50			
14	1.50	1.30	0.0350	
15	3.00			
16	0.50			
17	1.50	5.00		
18	3.00			
19	0.50			
20	1.50	0.50		
21	3.00			
22	0.50			
23	1.50	1.30	0.0500	
24	3.00			
25	0.50			
26	1.50	5.00		
27	3.00			
28	0.50			
29	1.50	0.50		
30	3.00			
31	0.50			
32	1.50	1.30	0.0254	
33	3.00			
34	0.50			
35	1.50	5.00		
36	3.00			
37	0.50			
38	1.50	0.50		
39	3.00			
40	0.50			
41	1.50	1.30	0.0350	pure water
42	3.00			
43	0.50			
44	1.50	5.00		
45	3.00			
46	0.50			
47	1.50	0.50		
48	3.00			
49	0.50			
50	1.50	1.30	0.0500	
51	3.00			
52	0.50			
53	1.50	5.00		
54	3.00			

Table 5. Matrix of 14 simulation cases upon varying the number of BHEs and BHEs connection (λ_{soil}=3.0 W/mK, λ_{grout}=5.0 W/mK, U-pipe spacing = 0.0500 m, mixture of water and ethylene glycol)

Simulation cases	Number of BHEs and BHEs connection (-)	Depth of boreholes (m)	BTES radius (m)
55	2 parallel-connected BHEs	49.73	1.67
56	2 series-connected BHEs	49.73	1.67
57	4 parallel-connected BHEs	24.87	2.36
58	4 series-connected BHEs	24.87	2.36
27	2 parallel-connected + 2 series-connected BHEs	24.87	2.36
59	6 parallel-connected BHEs	16.58	2.89
60	6 series-connected BHEs	16.58	2.89
61	3 parallel-connected + 3 series-connected BHEs	16.58	2.89
62	8 parallel-connected BHEs	12.43	3.34
63	8 series-connected BHEs	12.43	3.34
64	4 parallel-connected + 4 series-connected BHEs	12.43	3.34
65	10 parallel-connected BHEs	9.95	3.73
66	10 series-connected BHEs	9.95	3.73
67	5 parallel-connected + 5 series-connected BHEs	9.95	3.73

5.1 Energy analysis

The energy comparison between the proposed and conventional systems has been performed in terms of primary energy consumption by means of the index named Primary Energy Saving (PES) defined by Angrisani et al. [28]:

$$PES = \left(E_p^{CS} - E_p^{CSHPSS} \right) \Big/ E_p^{CS} \tag{7}$$

where, E_p^{CSHPSS} is the primary energy consumption of the proposed system and E_p^{CS} is the primary energy consumption of the conventional system. The values of E_p^{CSHPSS} and E_p^{CS} of Eq. 7 have been calculated based on the simulation results according to the following formulas:

$$E_p^{CSHPSS} = E_{th,MB}^{CSHPSS} \Big/ \eta_{MB} + E_{th,DHW}^{CSHPSS} \Big/ \eta_B + \left(E_{el,plant}^{CSHPSS} + E_{el,buildings}^{CSHPSS} \right) \Big/ \eta_{PP} \tag{8}$$

$$E_p^{CS} = \left(E_{th,Heating}^{CS} + E_{th,DHW}^{CS} \right) \Big/ \eta_B + E_{el,buildings}^{CS} \Big/ \eta_{PP} \tag{9}$$

where, $E_{th,MB}^{CSHPSS}$ is the thermal energy produced by the main back-up boiler for space heating purposes in the proposed system, $E_{th,DHW}^{CSHPSS}$ and $E_{th,DHW}^{CS}$ represent the thermal energy supplied by the individual boilers for DHW production in the proposed and conventional systems, respectively, $E_{th,Heating}^{CS}$ is the thermal energy required for heating purposes in the conventional system, $E_{el,plant}^{CSHPSS}$ represents the electric energy

consumption associated to all pumps and the heat dissipator of the plant in the proposed system, $E_{el,buildings}^{CSHPSS}$ and $E_{el,buildings}^{CS}$ represent the electric energy demands of buildings (due to lighting systems, domestic appliances, fan-coils and individual pumps) associated to the proposed and conventional system, respectively, η_{MB} is the efficiency of the main back-up boiler (Eq. 3), η_B is the efficiency of the individual boilers (assumed constant and equal to 90 %), η_{PP} is the power plant average efficiency in Italy, including transmission losses (assumed equal to 0.42 [28]).

5.2 Emissions analysis

The assessment of emissions has been performed in this study through the energy output-based emission factor approach suggested by Chicco and Mancarella [29]. In particular, the global carbon dioxide equivalent emissions associated to the operation of the systems have been compared by means of the following indicator ΔCO_2 [28]:

$$\Delta CO_2 = \left(m_{CO_2}^{CS} - m_{CO_2}^{CSHPSS} \right) \Big/ m_{CO_2}^{CS} \tag{10}$$

where, $m_{CO_2}^{CSHPSS}$ is the mass of global equivalent carbon dioxide emitted by the proposed system and $m_{CO_2}^{CS}$ is the mass of global equivalent carbon dioxide emitted by the conventional system. The values of $m_{CO_2}^{CSHPSS}$ and $m_{CO_2}^{CS}$ of Eq. 10 have been computed as suggested by Chicco and Mancarella [29]:

$$m_{CO_2}^{CSHPSS} = \beta \cdot \left(E_{th,MB}^{CSHPSS} \Big/ \eta_{MB} + E_{th,DHW}^{CSHPSS} \Big/ \eta_B \right) + \alpha \cdot \left(E_{el,plant}^{CSHPSS} + E_{el,buildings}^{CSHPSS} \right) \tag{11}$$

$$m_{CO_2}^{CS} = \beta \cdot \left(E_{th,Heating}^{CS} + E_{th,DHW}^{CS} \right) \Big/ \eta_B + \alpha \cdot E_{el,buildings}^{CS} \tag{12}$$

where, α is the CO_2 equivalent emission factor for electricity production, β represents the CO_2 equivalent emission factor associated to the consumption of natural gas. According to the values suggested in [28] for the Italian scenario, α has been assumed equal to 573 gCO_2/kWh_{el} and β has been considered of 207 gCO_2/kWh_p in this study.

5.3 Economic analysis

The economic analysis has been performed by comparing the operating costs of the proposed system with those associated to the reference heating system by means of the following parameter ΔOC suggested by Angrisani et al. [28]:

$$\Delta OC = \left(OC^{CS} - OC^{CSHPSS} \right) \Big/ OC^{CS} \tag{13}$$

where, OC^{CSHPSS} represents the operating costs of the proposed system and OC^{CS} represents the operating costs of the conventional system. The values of OC^{CS} and OC^{CSHPSS} of Eq. 13 have been calculated as follows:

$$OC^{CS} = UC_{ng} \cdot \frac{E_{th,Heating}^{CS} + E_{th,DHW}^{CS}}{LHV_{ng} \cdot \rho_{ng} \cdot \eta_B} + \\ + UC_{el} \cdot E_{el,buildings}^{CS} \qquad (14)$$

$$OC^{CSHPSS} = UC_{ng} \cdot \frac{E_{th,MB}^{CSHPSS}}{LHV_{ng} \cdot \rho_{ng} \cdot \eta_{MB}} + \\ + UC_{el} \cdot \left(E_{el,plant}^{CSHPSS} + E_{el,buildings}^{CSHPSS} \right) + UC_{ng} \cdot \frac{E_{th,DHW}^{CSHPSS}}{LHV_{ng} \cdot \rho_{ng} \cdot \eta_B} \qquad (15)$$

where, UC_{ng} is the unit cost of natural gas [30], LHV_{ng} is the lower heating value of natural gas (assumed equal to 49,599 kJ/kg), ρ_{ng} is the density of natural gas (assumed equal to 0.72 kg/m³), UC_{el} is the unit cost of electric energy purchased from the national central grid [30]. The tariffs of both electric energy as well as natural gas have been kept up-to-date according to the Italian scenario [30]. In particular, the values of UC_{el} range from 0.121 €/kWh to 0.301 €/kWh [30], while the values of UC_{ng} are the range between 0.466 €/Sm³ and 0.848 €/Sm³ [30] in Naples.

6. RESULTS AND DISCUSSION

In this section, the results associated to the simulation cases 1-67 described in Tables 4 and 5 are discussed and compared with those associated to the operation of the conventional heating system assumed as reference. The annual values of the primary energy consumption, the carbon dioxide equivalent emissions and the operating costs associated to the reference heating system are 60.69 MWh, 13.76 MgCO₂ and 4.65 k€, respectively. The performance of the CSHPSS varies year by year due to the presence and operation of the thermal energy storages. Figure 2 reports the values of PES (Eq. 7), ΔCO_2 (Eq. 10) and ΔOC (Eq. 13) as a function of the simulation year for the case 5. This figure highlights that the performances significantly improve from the 1st to the 3rd year of operation and then become substantially constant; this is thanks to the fact that the temperature in the BTES field mainly increase from the first to second year of operation, allowing for a more effective exploitation of solar energy; with respect to this last point, Figure 3 reports the temperature in the center of BTES field as a function of the time during 5 years for the simulation case 5.
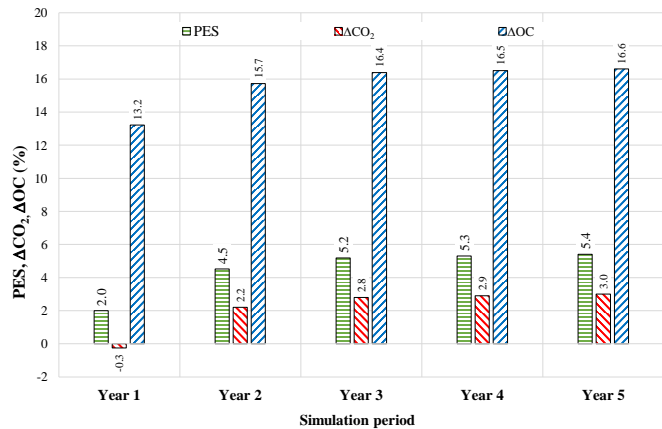

Figure 2. Values of PES, ΔCO_2 and ΔOC as a function of the year of operation for the simulation case 5
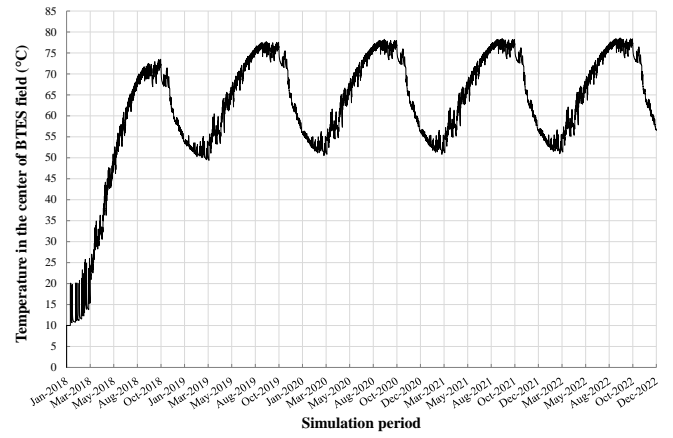

Figure 3. Temperature in the center of BTES as a function the time for the simulation case 5

Similar trends have been obtained for the other simulation cases, so that it can be stated that the behavior of the BTES becomes substantially stable after about two years (whatever the BTES configuration is). In the section 6.1 the effects of (i) thermal conductivity of soil, (ii) thermal conductivity of grout, (iii) U-pipe spacing and (iv) heat carrier fluid on the overall system performance are analyzed, while the impacts associated to both (i) the number of BHEs as well as (ii) the type of BHEs connection are described in the section 6.2.

6.1 Effects of thermo-physical properties of BTES

Figures 4a, 4b, 4c show the results associated to the simulation cases 1-54 (see Table 4), reporting the values of $PES^{5th-year}$, $\Delta CO_2^{5th-year}$ and $\Delta OC^{5th-year}$, respectively, referred to the 5th year of simulation as a function of thermal conductivity of soil (0.5, 1.5 and 3.0 W/mK), thermal conductivity of grout (0.5, 1.3 and 5.0 W/mK), U-pipe spacing (0.0254, 0.0350 and 0.0500 m) and heat carrier fluid (mixture of water and ethylene glycol or pure water). These figures highlight that: (a) the values of $PES^{5th-year}$, $\Delta CO_2^{5th-year}$ and $\Delta OC^{5th-year}$ are always positive, whatever the simulation case is; this means that the proposed plant is always able to reduce the primary energy consumption, the equivalent carbon dioxide emissions as well as the operating costs in comparison to the conventional heating plant, whatever the BTES characteristics are; (b) the values of $PES^{5th-year}$, $\Delta CO_2^{5th-year}$ and $\Delta OC^{5th-year}$ increase with the values of both λ_{soil} and λ_{grout}; (c) for given values of both λ_{grout} and U-pipe spacing, the values of $PES^{5th-year}$, $\Delta CO_2^{5th-year}$ and $\Delta OC^{5th-year}$ significantly increase up to 30 %, 58 % and 8 %, respectively, when λ_{soil} increases from 0.5 W/mK to 3.0 W/mK; (d) for given values of both λ_{soil} and U-pipe spacing, the values of $PES^{5th-year}$, $\Delta CO_2^{5th-year}$ and $\Delta OC^{5th-year}$ considerably improve by 63 %, 159 % and 15 %, respectively, when λ_{grout} rises from 0.5 W/mK to 5.0 W/mK; (e) for given values of λ_{soil} and λ_{grout}, the values of $PES^{5th-year}$, $\Delta CO_2^{5th-year}$ and $\Delta OC^{5th-year}$ slightly decrease by a variation in terms of U-pipe spacing from 0.0254 m to 0.0350 m; a small performance improvement is observed in the case of the U-pipe spacing increases from 0.0350 m to 0.0500 m; (f) the heat carrier fluid typology has a small impact in terms of $PES^{5th-year}$, $\Delta CO_2^{5th-year}$ and $\Delta OC^{5th-year}$; (g) with reference to the simulation cases 1-27 using a water/ethylene glycol mixture as heat carrier fluid, the best values of $PES^{5th-year}$ (6.96 %), $\Delta CO_2^{5th-year}$ (4.43 %) and $\Delta OC^{5th-year}$ (17.93 %) are obtained in the simulation case 27 (λ_{soil} = 3.00 W/mK, λ_{grout} = 5.00 W/mK, U-
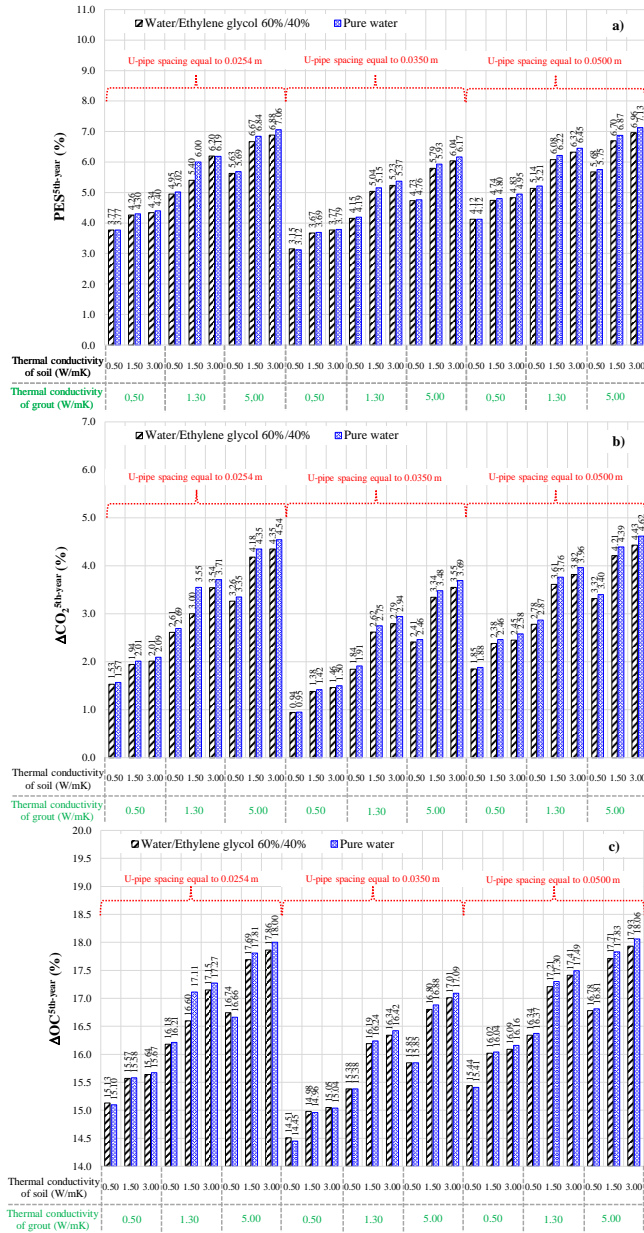
pipe spacing = 0.0500 m); (h) with reference to the simulation cases 28-54 using pure water as heat carrier fluid, the maximum values of $PES^{5th-year}$ (7.13 %), $\Delta CO_2^{5th-year}$ (4.62 %) and $\Delta OC^{5th-year}$ (18.06 %) are obtained in the simulation case 54 (λ_{soil} = 3.00 W/mK, λ_{grout} = 5.00 W/mK, U-pipe spacing = 0.0500 m).

Figure 4. Values of $PES^{5th-year}$ (a), $\Delta CO_2^{5th-year}$ (b) and $\Delta OC^{5th-year}$ (c) during the 5th year of simulation upon varying the thermal conductivity of soil and grout, U-pipe spacing and heat carrier fluid

The difference in terms of $PES^{5th-year}$, $\Delta CO_2^{5th-year}$ and $\Delta OC^{5th-year}$ between the configurations 27 (water/ethylene glycol mixture) and 54 (pure water) is almost negligible, so that the simulation case 27 can be assumed as the best case taking into account that the addition of glycol to water yields a solution with a freezing point below that of water, allowing to operate also when the outdoor temperature is lower than 0 °C.

Figures 5a, 5b and 5c report the main energy flows during the 5th year of operation associated to the main plant components as a function of λ_{soil}, λ_{grout} and U-pipe spacing, in the case of the mixture of water and ethylene glycol is used as heat carrier fluid.
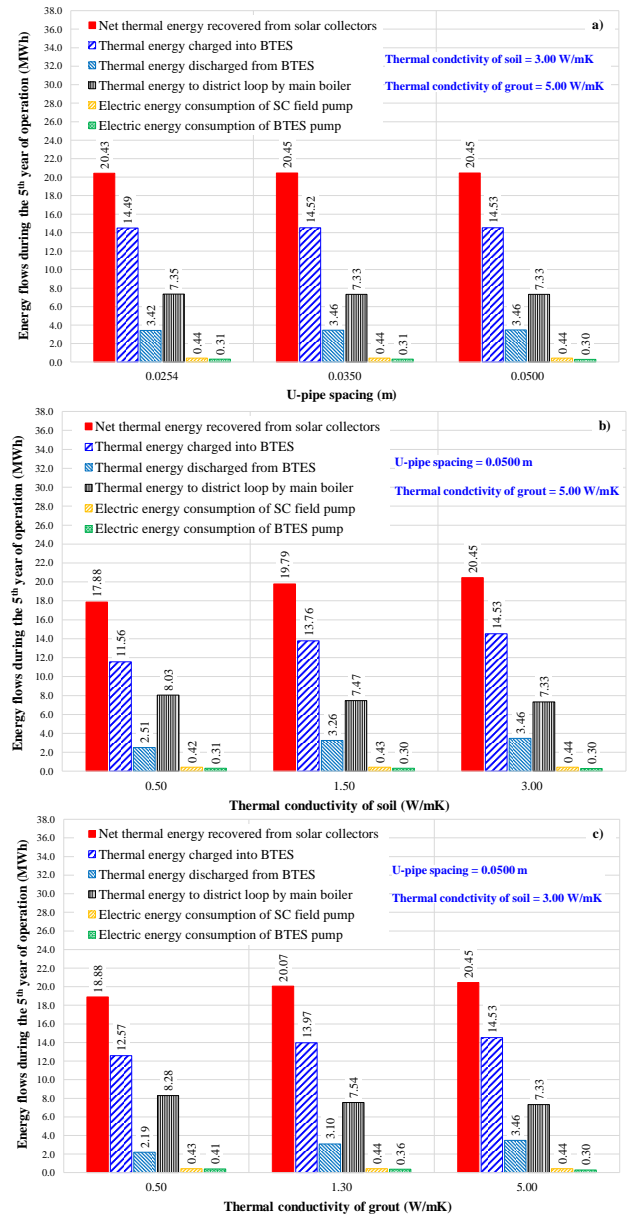

Figure 5. Energy flows associated to the main plant components as a function of U-pipe spacing (a), λ_{soil} (b) and λ_{grout} (c)

These figures show that: (a) for given values of λ_{soil} and λ_{grout}, the U-pipe spacing scarcely affects the performance of the BTES; (b) for given values of U-pipe spacing and λ_{grout}, in the case of λ_{soil} increases from 0.5 W/mK to 3.0 W/mK (i) the thermal energy recovered from solar collectors increases by about 14 %, (ii) the thermal energy injected into the BTES is enhanced by about 26 % and (iii) the thermal energy discharged from the BTES becomes about 38 % larger (together with a corresponding reduction of the thermal energy supplied by the boiler by around 9 %); (c) for given values of U-pipe spacing and λ_{soil}, when λ_{grout} increases from 0.5 W/mK to 5.0 W/mK (i) the thermal energy recovered from solar collectors increases by about 8 %, (ii) the thermal energy injected into the BTES becomes about 16 % greater and (iii) the thermal energy discharged from the BTES is enhanced by about 58 % (allowing for a reduction of thermal energy provided by the boiler by about 12 %).

6.2 Effects of BHEs arrangement

Figure 6 reports the values of PES, ΔCO_2 and ΔOC during the

5th year of operation as a function of the simulation cases 55-67 (see Table 5) characterized by a different (i) number of BHEs, and/or (ii) BHEs connection. The configurations 55-67 are characterized by the same λ_{soil} (3.0 W/mK), λ_{grout} (5.0 W/mK), U-pipe spacing (0.0500 m) and heat carrier fluid (mixture of water and ethylene glycol) of the simulation case 27 (recognized as the best configuration based on the analysis performed in the previous section 6.1).
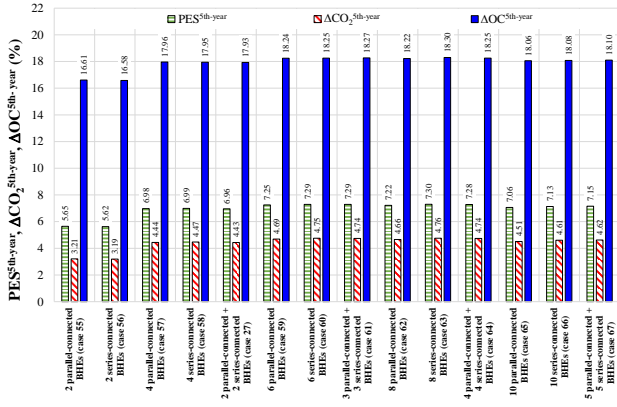

Figure 6. Values of PES, ΔCO_2 and ΔOC during the 5th year of operation as a function of BHEs arrangement

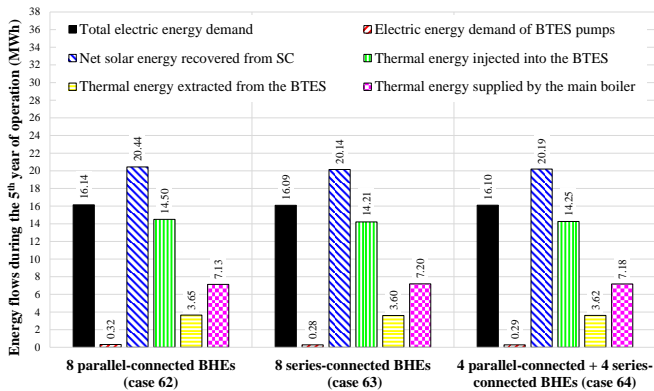**Figure 7.** Energy flows during the 5th year of operation for the configurations with 8 BHEs

Figure 6 shows that: (a) the values of PES$^{5th\text{-}year}$, $\Delta CO_2^{5th\text{-}year}$ and $\Delta OC^{5th\text{-}year}$ are always positive, whatever the simulation case is; this means that all the proposed configurations of the CSHPSS allow to always reduce the primary energy consumption, the equivalent CO_2 emissions as well as the operating costs in comparison to the reference heating system; (b) in the case of series-connected BHEs, the values of PES$^{5th\text{-}year}$, $\Delta CO_2^{5th\text{-}year}$ and $\Delta OC^{5th\text{-}year}$ increase with the number of BHEs up to reaching the maximum values when the number of borehole heat exchangers is equal to 8 and then slightly decrease. The maximum values of PES$^{5th\text{-}year}$ (7.30 %), $\Delta CO_2^{5th\text{-}year}$ (4.76 %) and $\Delta OC^{5th\text{-}year}$ (18.30 %) are obtained in the case with 8 series-connected boreholes (simulation case 63). Figure 7 reports the main energy flows associated to the proposed system during the 5th year of simulation for the cases of configurations with 8 boreholes; in particular, the total electric energy demand, the electric demand of BTES pump, the net solar energy recovered from solar collectors, the thermal energy injected/extracted into/from the BTES and the thermal energy supplied by the MB are reported. From this figure, it can be derived that, in comparison with the cases 62 (8 parallel-

connected BHEs) and 64 (4 parallel-connected + 4 series-connected BHEs), the configuration 63 with 8 series-connected BHEs is able to minimize the values of both total electric energy demand and electric energy consumption of BTES pumps; this allows to maximize the potential savings in terms of primary energy consumption, carbon dioxide equivalent emissions and operating costs (even if, in comparison to the cases 62 and 64, the solar energy extracted from the BTES is slightly lower and the thermal energy supplied by the boiler is a bit greater).

7. CONCLUSION

A parametric analysis has been performed in order to investigate the performance of a centralized hybrid solar district heating network integrated with a seasonal borehole thermal energy storage upon varying the (i) thermal conductivity of soil, (ii) thermal conductivity of grout, (iii) U-pipe spacing, (iv) heat carrier fluid, (v) number of BHEs as well as (vi) type of BHEs connection (series, parallel o mixed). The simulation results highlighted that: (a) the proposed system is always able to reduce the primary energy consumption (up to 7.30 %), carbon dioxide emissions (up to 4.76 %) and operating costs (up to 18.30 %) in comparison to a conventional Italian decentralized heating system, whatever the CSHPSS configuration is; (b) the values of PES$^{5th\text{-}year}$, $\Delta CO_2^{5th\text{-}year}$ and $\Delta OC^{5th\text{-}year}$ significantly increase with the thermal conductivity of both grout and soil; (c) the U-pipe spacing a well as the heat carrier fluid have a negligible influence on the overall performance of the district heating network; (d) for a given type of BHEs connection, the values of PES$^{5th\text{-}year}$, $\Delta CO_2^{5th\text{-}year}$ and $\Delta OC^{5th\text{-}year}$ increase with the number of BHEs up to reaching the maximum values in the case of the number of borehole heat exchangers is equal to 8 and then slightly decrease; (e) for a given number of BHEs, the values of PES$^{5th\text{-}year}$, $\Delta CO_2^{5th\text{-}year}$ and $\Delta OC^{5th\text{-}year}$ are maximized in the cases of the boreholes are series-connected, even if the effects of BHEs connection is not particularly significant.

REFERENCES

[1] Rad, F.M., Fung, A.S. (2016). Solar community heating and cooling system with borehole thermal energy storage–Review of systems. Renewable and Sustainable Energy Reviews, 60: 1550-1561. https://doi.org/10.1016/j.rser.2016.03.025

[2] Carpaneto, E., Lazzeroni, P., Repetto, M. (2015). Optimal integration of solar energy in a district heating network. Renewable Energy, 75: 714-721. https://doi.org/10.1016/j.renene.2014.10.055

[3] Xu, J., Wang, R. Z., Li, Y. (2014). A review of available technologies for seasonal thermal energy storage. Solar Energy, 103: 610-638.

https://doi.org/10.1016/j.solener.2013.06.006

[4] Hesaraki, A., Holmberg, S., Haghighat, F. (2015). Seasonal thermal energy storage with heat pumps and low temperatures in building projects—A comparative review. Renewable and Sustainable Energy Reviews, 43: 1199-1213. https://doi.org/10.1016/j.rser.2014.12.002

[5] Flynn, C., Sirén, K. (2015). Influence of location and design on the performance of a solar district heating system equipped with borehole seasonal storage. Renewable Energy, 81: 377-388. https://doi.org/10.1016/j.renene.2015.03.036

[6] IEA-SHC. IEA-SHC - Task 32 - Advanced storage concepts for solar and low energy buildings' n.d. http://task32.iea-shc.org/ (accessed May 20, 2020).

[7] IEA SHC. IEA SHC - Task 45 - Large Systems: Large Solar Heating/Cooling Systems, Seasonal Storage, Heat Pumps n.d. http://task45.iea-shc.org/ (accessed May 20, 2020).

[8] Lottner, V., Schulz, M. E., Hahne, E. (2000). Solar-assisted district heating plants: Status of the German programme Solarthermie-2000. Solar Energy, 69(6): 449-459. https://doi.org/10.1016/S0038-092X(00)00125-0

[9] Wołoszyn, J., Gołaś, A. (2014). Sensitivity analysis of efficiency thermal energy storage on selected rock mass and grout parameters using design of experiment method. Energy Conversion and Management, 87: 1297-1304. https://doi.org/10.1016/j.enconman.2014.03.059

[10] Talebi, B., Haghighat, F., Tuohy, P., Mirzaei, P.A. (2019). Optimization of a hybrid community district heating system integrated with thermal energy storage system. Journal of Energy Storage, 23: 128-137. https://doi.org/10.1016/j.est.2019.03.006

[11] Barberis, S., Rivarolo, M., Traverso, A., Massardo, A.F. (2016). Thermo-economic analysis of the energy storage role in a real polygenerative district. Journal of Energy Storage, 5: 187-202. https://doi.org/10.1016/j.est.2016.01.001

[12] Zanghirella, F., Canonaco, J., Puglisi, G., Di Pietra, B. (2016). Introducing solar thermal "net metering" in an actual small-scale district heating system: A case-study analysis. Energy Procedia, 101: 240-248. https://doi.org/10.1016/j.egypro.2016.11.031

[13] Carotenuto, A., Figaj, R.D., Vanoli, L. (2017). A novel solar-geothermal district heating, cooling and domestic hot water system: Dynamic simulation and energy-economic analysis. Energy, 141: 2652-2669. https://doi.org/10.1016/j.energy.2017.08.084

[14] Di Pietra, B., Zanghirella, F., Puglisi, G. (2015). An evaluation of distributed solar thermal "net metering" in small-scale district heating systems. Energy Procedia, 78: 1859-1864. https://doi.org/10.1016/j.egypro.2015.11.335

[15] Buoro, D., Pinamonti, P., Reini, M. (2014). Optimization of a Distributed Cogeneration System with solar district heating. Applied Energy, 124: 298-308. https://doi.org/10.1016/j.apenergy.2014.02.062

[16] Panno, D., Buscemi, A., Beccali, M., Chiaruzzi, C., Cipriani, G., Ciulla, G., Bonomolo, M. (2019). A solar assisted seasonal borehole thermal energy system for a non-residential building in the Mediterranean area. Solar Energy, 192: 120-132. https://doi.org/10.1016/j.solener.2018.06.014

[17] TRNSYS. The transient energy system simulation tool n.d. http://www.trnsys.com

[18] Ciampi, G., Rosato, A., Sibilio, S. (2018). Thermo-economic sensitivity analysis by dynamic simulations of a small Italian solar district heating system with a seasonal borehole thermal energy storage. Energy, 143: 757-771. https://doi.org/10.1016/j.energy.2017.11.029

[19] Richardson, I., Thomson, M., Infield, D., Clifford, C. (2010). Domestic electricity use: A high-resolution energy demand model. Energy and Buildings, 42(10): 1878-1887. https://doi.org/10.1016/j.enbuild.2010.05.023

[20] Jordan, U., Vajen, K. (2001). Realistic Domestic Hot-Water Profiles in Different Time Scales.

[21] Kloben. FSK model n.d. http://www.kloben.it/products/view/3 (accessed January 13, 2020).

[22] Paradigma. PS series n.d. http://www.paradigmaitalia.it/serbatoio-accumulo-acqua-calda-riscaldamento/boiler-accumulo-acqua-calda/accumulo-solare-termico.

[23] Vaillant. atmoTEC exclusive VMW n.d. https://www.vaillant.it/home/prodotti/atmotec-exclusive-vmw-9664.html.

[24] Hellström, G. (1989). Heat Storage in the Ground, Duct ground heat storage model, Manual for Computer Code. Department of Mathematical Physics, University of Lund, Box 118, S-221 00 Lund, Sweden.

[25] Pahud, D. (2000). Central solar heating plants with seasonal duct storage and short-term water storage: design guidelines obtained by dynamic system simulations. Solar Energy, 69(6): 495-509. https://doi.org/10.1016/S0038-092X(00)00119-5

[26] EnergyPlus. Weather data, EnergyPlus energy simulation software n.d. http://apps1.eere.energy.gov/buildings/energyplus.

[27] Casasso, A., Sethi, R. (2014). Sensitivity analysis on the performance of a ground source heat pump equipped with a double U-pipe borehole heat exchanger. Energy Procedia, 59: 301-308. https://doi.org/10.1016/j.egypro.2014.10.381

[28] Angrisani, G., Canelli, M., Roselli, C., Russo, A., Sasso, M., Tariello, F. (2017). A small scale polygeneration system based on compression/absorption heat pump. Applied Thermal Engineering, 114: 1393-1402. https://doi.org/10.1016/j.applthermaleng.2016.10.048

[29] Chicco, G., Mancarella, P. (2008). Assessment of the greenhouse gas emissions from cogeneration and trigeneration systems. Part I: Models and indicators. Energy, 33(3): 410-417. https://doi.org/10.1016/j.energy.2007.10.006

[30] ARERA, Italian Regulatory Authority for Energy, Networks and Environment n.d. https://www.arera.it/it/inglese/index.htm.